Multiscale Investigation of the Depth-Dependent Mechanical Anisotropy of the Human Corneal Stroma

Cristina Labate,[1] Marco Lombardo,[2] Maria P. De Santo,[1] Janice Dias,[3] Noel M. Ziebarth,[3] and Giuseppe Lombardo[4,5]

[1]Department of Physics, University of Calabria, Rende, Italy
[2]Fondazione G.B. Bietti IRCCS, Rome, Italy
[3]Biomedical Atomic Force Microscopy Laboratory, Department of Biomedical Engineering, University of Miami College of Engineering, Coral Gables, Florida, United States
[4]Consiglio Nazionale delle Ricerche, Istituto per i Processi Chimico-Fisici (CNR-IPCF), Messina, Italy
[5]Vision Engineering Italy srl, Rome, Italy

Purpose. To investigate the depth-dependent mechanical anisotropy of the human corneal stroma at the tissue (stroma) and molecular (collagen) level by using atomic force microscopy (AFM).

Methods. Eleven human donor corneas were dissected at different stromal depths by using a microkeratome. Mechanical measurements were performed in 15% dextran on the surface of the exposed stroma of each sample by using a custom-built AFM in force spectroscopy mode using both microspherical (38-µm diameter) and nanoconical (10-nm radius of curvature) indenters at 2-µm/s and 15-µm/s indentation rates. Young's modulus was determined by fitting force curve data using the Hertz and Hertz-Sneddon models for a spherical and a conical indenter, respectively. The depth-dependent anisotropy of stromal elasticity was correlated with images of the corneal stroma acquired by two-photon microscopy.

Results. The force curves were obtained at stromal depths ranging from 59 to 218 µm. At the tissue level, Young's modulus (E_S) showed a steep decrease at approximately 140-µm stromal depth (from 0.8 MPa to 0.3 MPa; $P = 0.03$) and then was stable in the posterior stroma. At the molecular level, Young's modulus (E_C) was significantly greater than at the tissue level; E_C decreased nonlinearly with increasing stromal depth from 3.9 to 2.6 MPa ($P = 0.04$). The variation of microstructure through the thickness correlated highly with a nonconstant profile of the mechanical properties in the stroma.

Conclusions. The corneal stroma exhibits unique anisotropic elastic behavior at the tissue and molecular levels. This knowledge may benefit modeling of corneal behavior and help in the development of biomimetic materials.

Keywords: atomic force microscopy, elasticity, anisotropy, microscopy

The histology and, accordingly, biomechanics of the human corneal stroma are highly heterogeneous. There is extensive knowledge on the existence of regional differences in the collagen fibril bundles' packing arrangement and lamellar orientation across and throughout the thickness of the human corneal stroma.[1-5] The anterior stroma consists of short bundles of collagen fibrils that show dense intertwining and also insert vertically into Bowman's layer, thus contributing to maintain corneal shape. The deeper stroma contains collagen fibril bundles that are arranged in wide lamellae oriented predominantly along the superior/inferior and nasal/temporal meridians and with reduced connections between adjacent layers.

Several laboratory techniques have been used to elucidate the depth-dependent mechanical properties of the human corneal stroma.[6-17] All of these studies have shown that the elastic modulus within the stroma decreases from anterior to posterior, regardless of the mechanical testing used. It is therefore well accepted that the depth-dependent changes of stromal mechanical elasticity are linked to the depth-dependent change of stromal microstructure.

Atomic force microscopy (AFM) enables localized mechanical sample testing and has been used to investigate the local elastic modulus of the human corneal stroma at different depths. Although the results from previous studies[6-11] could not be directly compared, because of the use of AFM tips with variable geometry and dimension as well as different study protocols, the elastic modulus is shown to decrease 40% to 80% with depth from the anterior stroma to the posterior part of the stroma.

The aim of this study was to provide information on the depth-dependent compressive elastic modulus of the human corneal stroma both at the tissue (stroma) and molecular (collagen) level by using AFM. In addition, we correlated the depth-dependent anisotropy of stromal elasticity with images of the human corneal stroma acquired by second harmonic generation (SHG) microscopy.

MATERIALS AND METHODS

Corneal Tissues

Donor human eye globes ($n = 11$; age range, 19–92 years; postmortem interval range, 2.5–12.1 hours) were obtained from the Florida Lions Eye Bank (Miami, FL, USA) in sealed vials with gauze soaked in balanced salt solution. The whole globes were in these vials from the time of extraction until the time of receipt (within 5 days) at the Biomedical Atomic Force Microscopy Laboratory of the University of Miami. Donors did not have history of corneal pathologies or eye surgery. All human eyes were obtained and used in compliance with the guidelines of the Declaration of Helsinki for research involving the use of human tissue. Immediately upon arrival in the laboratory, the corneal epithelium was removed by using a cotton-tipped applicator, and pachymetry measurements were taken to determine extent of corneal swelling. The whole globes were submerged in 20% dextran solution, cornea side down, to restore corneal thickness to physiological levels. The whole globes remained in the 20% dextran solution for 24 hours in the refrigerator at 4°C. The corneas were excised from the whole globe after this pretreatment with 20% dextran. Before AFM mechanical testing, pachymetry measurements were performed by using an ultrasound pachymeter (DGH 55 Pachmate; DGH Technology, Inc., Exton, PA, USA) to ensure that the central corneal thickness was within the physiological range of 400 to 600 μm. Each sample was mounted onto an artificial chamber and a microkeratome (CB, Moria, France) with two different microkeratome heads of 50- and 90-μm depth was used to dissect the cornea at different stromal depths. The pressure inside the artificial anterior chamber was not monitored during the microkeratome cut in order to achieve different cutting depths in each corneal sample. The anterior corneal flap created by the microkeratome was discarded and the biomechanical properties of each specimen were measured by indenting the surface of the exposed stroma of the posterior lenticule.

Three additional sclerocorneal tissues, from different donors, not suitable for transplantation, were obtained from the Veneto Eye Bank Foundation (Venezia Zelarino, Italy) and used for SHG microscopy imaging at the Department of Physics of the University of Calabria. Tissues were used in compliance with the guidelines of the Declaration of Helsinki for research involving the use of human tissue and the experimental protocol was approved by the National Research Council research ethics and bioethics advisory committee. Donors did not have history of corneal pathologies or eye surgery.

Atomic Force Microscopy Data Acquisition

The mechanical properties of the corneal stroma were investigated by using a custom-built AFM in force spectroscopy mode.[7,10,18] Each posterior stromal lenticule was placed, facing upward, in a sample holder and maintained in place without the use of glue.[7,10] Measurements were performed with the samples immersed in 15% dextran solution, which has been found in a previous study to be the most effective solution in maintaining corneal hydration and Young's modulus over time.[19]

Both microsized and nanosized AFM tips were used to measure the depth-dependent mechanical anisotropy of the stroma at the tissue and individual tissue component (ie, collagen) levels, respectively. Tipless AFM cantilevers (nominal spring constant: 4.5 N/m, NSC12 series; Mikromasch, San Jose, CA, USA) were modified with glass microspheres (30–50 μm nominal diameter; Polysciences, Inc., Warrington, PA, USA) by using epoxy adhesive.[7,10,19] The cantilevers were allowed to

dry overnight and then rinsed in ethanol to remove the excess epoxy. Each cantilever was then calibrated to determine its spring constant by using a reference force calibration cantilever (nominal spring constant: 10.4 N/m, CLFC-NOBO; Bruker, Camarillo, CA, USA) manufactured specifically for the calibration of other probes.[7,10,20] This method was based on the "beam on beam" approach developed by Gibson et al.[21] and Tortonese and Kirk,[22] in which a cantilever of unknown spring constant is brought into contact with a calibrated standard cantilever beam. Twenty force curves were recorded on different locations at the center of the stromal surface of the posterior lenticule at two different approach speeds, 2 μm/s ($n = 5$) and 15 μm/s ($n = 11$) in order to investigate the different behavior of the corneal stroma under "slow" and "fast" indentation rates.[9]

Commercially available phosphorus-doped rectangular silicon cantilever of nominal elastic constant between 20 and 80 N/m (TESPA; Bruker) with 10-nm radius of curvature tips was used in four specimens. The cantilever elastic constant was calculated by using its geometric dimensions, as described in previous work[23]:

$$k = \frac{3E_k I}{L^3}, \qquad (1)$$

where L is the length of the cantilever, E_k is the lever Young's modulus, and I is the moment of inertia of a trapezoidal section cantilever. Twenty force curves were recorded at 2-μm/s ($n = 4$) and 15-μm/s ($n = 4$) indentation rates on different locations at the center of the stromal surface of each posterior lenticule collected from different donors.

Atomic Force Microscopy Data Analysis

The optical detector sensitivity was measured as the slope of the force curve in 15% dextran, when the tip was in contact with a rigid surface, in this case a Petri dish; this value was used to convert the cantilever deflection, in volts, to deflection in micrometers by using a specifically written routine in Matlab (version 2013; The Mathworks, Inc., Natick, MA, USA). We made sure that the same conditions were kept during the experiment. At the end of every set of force measurements, we acquired an additional reference force measurement on the hard surface to verify that the calibration was not changed during the experiment.[9] The program was further customized to automatically detect the contact point between the tip and the stromal surface. The search for contact point was performed on both the approaching and retracting curves. As an example, the first derivative of the approach curve was calculated and the contact point was chosen in the range where the derivative started to be different from zero. Thereafter, the approach and retract curves were shifted with respect to the calculated contact point before estimation of the Young's modulus.

Young's modulus of elasticity was calculated for each cornea individually by using the data obtained by either microspherical or nanoconical AFM indenters. The automatic detection of the contact point provided highly reproducible values of modulus of elasticity.[9] For microspherical tips, the Young's modulus was determined by fitting force curve data (ie, the fit was done, from the contact point, on the entire approach curve) to the Hertz model for a spherical indenter[7,10]:

$$F = F_0 + \frac{4E_S \sqrt{R}}{3(1 - v^2)}(\delta - \delta_0)^{\frac{3}{2}}, \qquad (2)$$

where F_0 and δ_0 are the loading force at baseline and the indentation depth at the contact point, v is Poisson's ratio (0.49 to indicate near incompressibility for the corneal tissue),[23] δ is

the indentation depth, and E_S is the Young's modulus of the stroma (in Pascal) and R is the radius of the spherical tip.

For nanoconical tips, the Young's modulus was calculated by using the Hertz-Sneddon model (the fit was done, from the contact point, on the entire approach curve)[9,24]:

$$F = F_0 + \frac{2}{\pi}\frac{E_C}{1 - v^2}(\delta - \delta_0)^2 tan\alpha, \qquad (3)$$

where α is the semi-opening angle of the conical tip (17.5°) and E_C is the Young's modulus of the stromal collagen. For both types of AFM indenters, a nonlinear least square curve fitting method was applied to the approach part of the force curve.

Second Harmonic Generation Microscopy

Three eye bank donor sclerocorneal tissues were imaged by using two-photon microscopy (Leica DM6000CS; Leica Microsystems GmbH, Wetzlar, Germany). The samples were placed on a glass slide under an upright microscope and illuminated with a pulse width of 140 fs (measured at the sample plane) at 80 MHz of repetition rate generated by a Ti:Sapphire laser (Vision II; Coherent, Santa Clara, CA, USA) tuned to 810 nm. The laser power was attenuated by an electro-optical-modulator (EOM) and then coupled into the Leica SP8-Spectral Scan-Head (Leica Microsystems GmbH) where it passes through the x–y scanning mechanism before being focused by a Leica HCX IRAPO 25x/0.95 NA IRAPO water immersion objective (2.5-mm working distance). Second harmonic generation signal was collected in forward direction by a nondescanned detector. Forward scatter signals that passed through the sample were collected with the use of a short pass filter ($\lambda < 680$ nm, SP680) and a 10-nm full width at half maximum (FWHM) band pass filter centered at 405 nm (FF01-405/10-25; Semrock, Inc., Rochester, NY, USA) positioned in front of the transmission light detector.

The samples were mounted with the corneal surface parallel to the scanning plane and were scanned with a 2- and 5-μm step size in the z-axis, extending from the surface of Bowman's layer to the endothelium. Image recording was performed on multiple locations in the central region of each tissue. Image processing, analysis, and visualization were carried out by using proprietary Leica software and an image processing package (Rasband WS, ImageJ; http://imagej.nih.gov/ij/; provided in the public domain by the National Institutes of Health, Bethesda, MD, USA) using custom-written macros. The stacks of SHG images were used to reconstruct cross-sectional images of the stroma.

Statistics

A commercial software program (KyPlot; KyensLab, Inc., Tokyo, Japan) was used for statistical testing. Data were given as mean ± standard deviation. The Wilcoxon test was used to statistically compare either E_S or E_C values between the anterior stroma (defined as the anterior 140 μm in this study based on the results of SHG imaging of the stroma) and the posterior stroma (corresponding to the remaining depth), E_S or E_C values obtained at the two different approach speeds, and E_S and E_C values obtained at the two different scales. The differences with a P value of 0.05 or less were considered statistically significant.

RESULTS

The central corneal thickness of corneal specimens ranged between 514 and 596 μm (average, 554 ± 27 μm). The force curves were obtained at stromal depths ranging from 59 to

TABLE 1. Human Cornea Sample Information

Sample	Cornea 1_OD	Cornea 1_OS	Cornea 2	Cornea 3_OD	Cornea 4_OD	Cornea 5	Cornea 4_OS	Cornea 6	Cornea 3_OS	Cornea 7	Cornea 8
Donor age, y	92	92	81	19	62	73	62	22	19	81	22
Stromal depth, μm	59	73	82	127	136	137	147	174	202	205	218
Young's modulus at 15-μm/s approach speed, MPa	0.99 ± 0.12	0.90 ± 0.03	0.91 ± 0.05	1.03 ± 0.21	0.20 ± 0.01	0.71 ± 0.05	0.22 ± 0.02	0.20 ± 0.03	0.17 ± 0.01	0.65 ± 0.08	0.41 ± 0.04
Young's modulus at 2-μm/s approach speed, MPa	0.55 ± 0.04	0.56 ± 0.04	0.35 ± 0.04	-	-	0.35 ± 0.04	-	-	-	0.20 ± 0.03	-

The donor age, stromal depth, and Young's modulus of elasticity (MPa) evaluated by using a microspherical AFM indenter (38-μm diameter) at two different approach speeds. Values for the modulus of elasticity are average ± standard deviation. OD, oculus dexter; OS, oculus sinister.
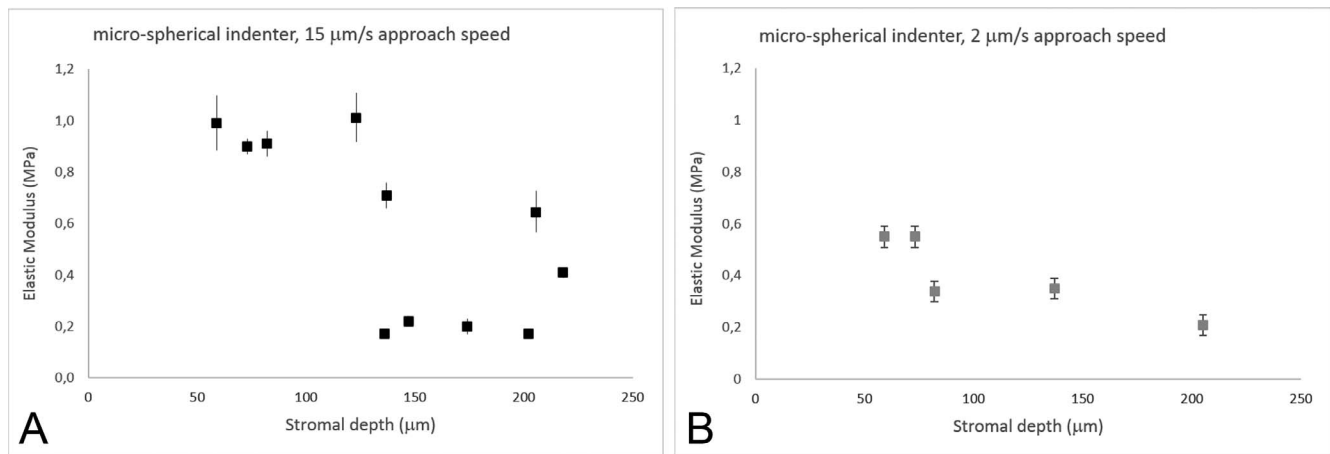
Figure 1. (A) Young's modulus of elasticity (E_S, MPa) as a function of stromal depth. Data ($n = 11$) were collected with a microspherical indenter at 15-μm/s approach speed. E_S decreased as a function of stromal depth, with a steep drop at 140-μm depth ($y = -0.56\ln(x) + 3.30$; $R^2 = 0.56$). *Vertical bars* indicate standard deviation. (B) E_S values from five samples were collected with a microspherical indenter at 2-μm/s approach speed. At a slow scan speed, the elastic modulus shows a staircase decrease with increasing stromal depth ($y = -0.26\ln(x) + 1.62$; $R^2 = 0.80$). *Vertical bars* indicate standard deviation. At the tissue level, E_S values obtained at 2-μm/s approach speed were 39% to 59% lower than at 15 μm/s. The differences increased with increasing stromal depth.

218 μm (Table 1). Three pairs of samples, that is, samples n.1, n.3, and n.4, were collected from the same donors.

Corneal Stroma Elasticity at the Tissue Level

An AFM cantilever modified with a 38-μm-diameter glass microsphere was used to probe the mechanical properties of 11 samples at the tissue level. The elastic constant of the lever was 15.1 N/m. No adhesion was detected between the microspherical tip and stromal surface.

At 15-μm/s approach speed, the Young's modulus (E_S) decreased as a function of stromal depth (Fig. 1; Table 1). The elastic modulus was stable in the most anterior 140-μm stroma, then it decreased by three times in the posterior stroma ($P = 0.03$; Fig. 1A). On average, the Young's modulus of the stroma varied from 0.80 ± 0.04 MPa in the anterior 140-μm depth to 0.33 ± 0.03 MPa in the posterior stroma (>140-μm depth).

In 5 of these 11 corneal specimens, measurements were also acquired at 2-μm/s approach speed. Overall, the values of Young's modulus of elasticity were 39% to 69% lower than the values measured at 15-μm/s approach speed ($P = 0.01$; Table 1). The Young's modulus of elasticity decreased with increasing stromal depths, showing two steps, at 80- and 200-μm depth (Fig. 1B). On average, the Young's modulus of the stroma varied from 0.55 ± 0.04 MPa in the anterior 80-μm depth to 0.20 ± 0.03 MPa in the posterior stroma (>140-μm depth).

The average indentation depth ranged from 2.6 ± 0.7 μm in the anterior 140-μm stroma to 3.4 ± 0.8 μm in the posterior stroma. No significant differences ($P = 0.65$) were found between the two indentation rates used.

Corneal Stroma Elasticity at the Molecular Level

An AFM cantilever with an elastic constant of 40 N/m and a tip with a nominal radius of curvature of 10 nm were used to evaluate the mechanical properties of the corneal tissue at the molecular level. No adhesion was found between the nanoconical tip and stromal surface.

Experiments were performed on four human donor corneas at 2-μm/s and 15-μm/s approach speeds (Table 2). At 15-μm/s approach speed, the Young's modulus decreased nonlinearly with increasing stromal depths, though the depth-dependent differences were less pronounced than using microspherical tips (Fig. 2A). The E_C values of the anterior 140-μm stroma were two times greater than the deeper stroma ($P = 0.04$); they ranged between 3.99 and 2.23 MPa across stromal depth. No significant differences ($P = 0.08$) were found between E_C values obtained at 2 μm/s and 15 μm/s; these differences ranged between 1% and 13% from the anterior to posterior stroma (Fig. 2B). On average, the indentation depth ranged from 3.3 ± 0.3 to 4.2 ± 0.7 μm from the anterior 140 μm to posterior stroma, with no differences between the two indentation rates ($P = 0.52$).

In the four tissues probed with both microspherical and nanoconical indenters, the E_C values were approximately 4 ($P = 0.02$) and 10 ($P = 0.003$) times greater than E_S values at 2-μm/s and 15-μm/s approach speeds, respectively (Tables 1 and 2).

Second Harmonic Generation Microscopy Imaging

A microstructural gradient from the anterior to posterior regions was found across the human corneal stroma; the collagen fibril bundles' packing and organization changed

TABLE 2. Young's Modulus of Elasticity (MPa) Evaluated With a Nanoconical AFM Tip (10-nm Radius of Curvature) at Two Different Approach Speeds

Sample	Cornea 2	Cornea 3_OD	Cornea 5	Cornea 7
Donor age, y	81	19	73	81
Stromal depth, μm	82	127	137	205
Young's modulus at 15-μm/s approach speed, MPa	3.99 ± 0.63	2.87 ± 0.61	2.94 ± 0.43	2.57 ± 0.26
Young's modulus at 2-μm/s approach speed, MPa	3.88 ± 0.55	2.70 ± 0.56	2.90 ± 0.77	2.23 ± 0.65

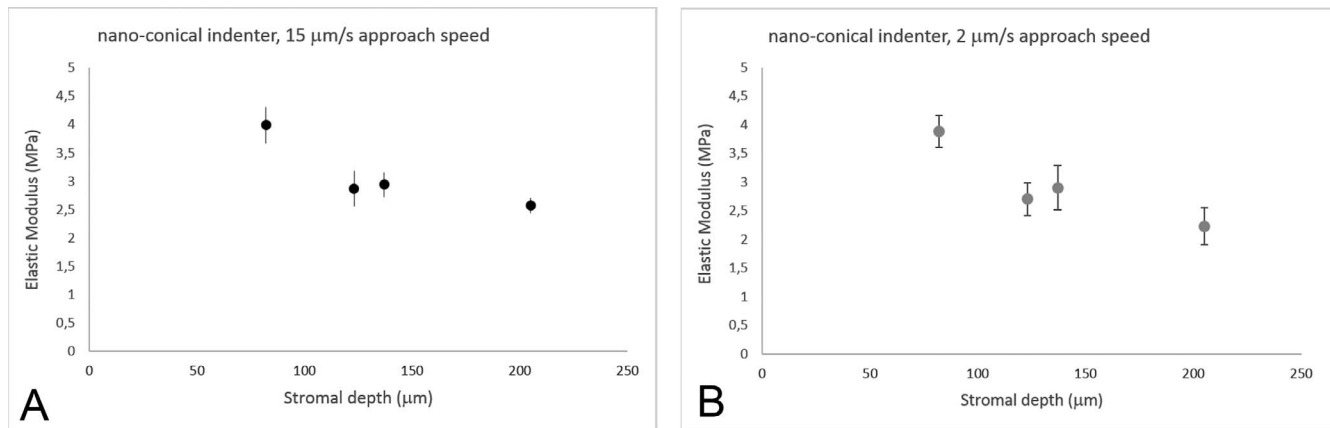Values for the modulus of elasticity are average ± standard deviation.

FIGURE 2. **(A)** Young's modulus of elasticity (E_C, MPa) as a function of stromal depth. Data ($n = 4$) were collected with a nanoconical indenter at 15-μm/s approach speed. The modulus of elasticity showed a logarithmic decrease with increasing depth ($y = -1.52\ln(x) + 10.49$; $R^2 = 0.86$). *Vertical bars* indicate standard deviation. **(B)** E_C values from each sample ($n = 4$) were also collected with a nanoconical indenter at 2-μm/s approach speed. The modulus of elasticity showed logarithmic decrease with increasing depth ($y = 1.75\ln(x) + 11.45$; $R^2 = 0.90$). *Vertical bars* indicate standard deviation. At the molecular level, E_C showed slight differences, ranging between 1% and 12%, between the two indentation rates used in this study; the differences increased with increasing stromal depth.

consistently with depth. The most anterior portion, up to 70 μm, showed numerous tiny and short bundles of collagen fibril bundles intertwining at apparently random angles and intersecting and/or fusing together at different planes. Several fibril bundles crossed the stroma vertically inserting into Bowman's layer (Fig. 3). The structural organization of collagen fibril bundles showed to change across 130- and 190-μm depth, in which they were organized in thin and densely packed lamellae (Figs. 4A–D). In the mid stroma (>200 μm; Figs. 4E–F), the collagen fibril bundles were organized in lamellae that became larger with increasing depth. The posterior region (>350 μm; Figs. 4G–H) was primarily composed of wide collagen lamellae aligned parallel to the corneal surface, forming a grid-like lamellar structure in the central region of the stroma.

DISCUSSION

Atomic force microscopy was used to investigate the elastic properties of the human corneal stroma by using 38-μm-diameter spherical and 10-nm-radius-of-curvature conical indenters. The use of microbeads, by increasing the surface contact area, enables networks of the stromal microstructure to be mechanically probed rather than individual collagen components of the stroma, as is done by using nanosized tips.

At the tissue level, Young's modulus of elasticity decreased nonlinearly with increasing depth. At 15-μm/s approach speed, it showed a steep decrease (⅔ lower) at approximately 140-μm stromal depth and then it was stable across the deeper stroma. In the most anterior stromal layers (≤140 μm), E_S was averagely 0.8 MPa, decreasing to 0.3 MPa at stromal depths deeper than 140 μm. At 2-μm/s approach speed, E_S showed a staircase decrease (up to –60%) from the most anterior stromal layers to the deeper stroma, presenting two steps at 80- and 200-μm depth.

The values of Young's modulus of elasticity at 2-μm/s approach speed were ⅓ to ½ significantly lower than those at 15-μm/s approach speed in each sample. This was consistent with the mechanical behavior of a viscoelastic material. In previous studies,[9,25,26] a nonlinear adaptation of the anterior stromal microstructure in relation to the speed of the local applied deformation has been shown, using indentation techniques either at the molecular or tissue level, likely due to less fluid movement and stretching between collagen fibril bundles and/or extracellular matrix (ECM) components. Previous studies have demonstrated that the nonlinear stress–strain response of the human cornea is rate dependent, characterized by increasing stiffness with increasing loading
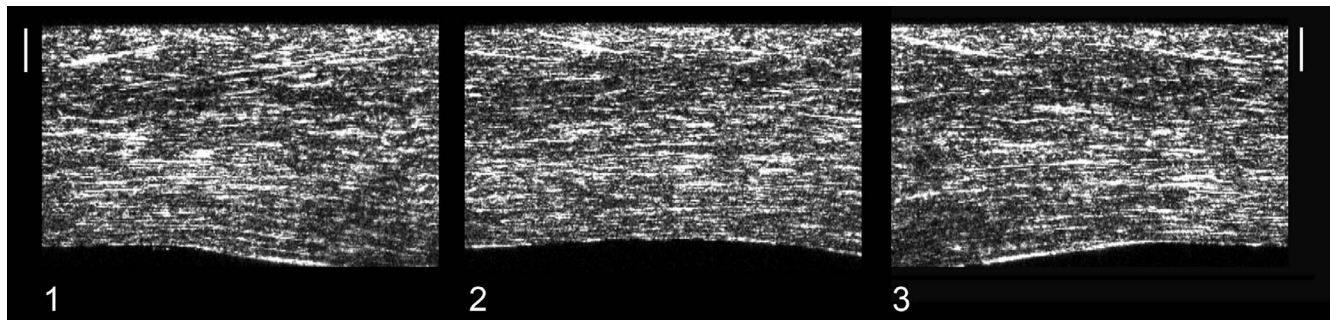

FIGURE 3. The stacks of SHG images were used to form cross-sectional images of the whole corneal stroma. The three corneal samples ([1], [2], and [3]) were scanned with a 2-μm step size in the *z*-axis, extending from the surface of Bowman's layer to the endothelium. The epithelium was removed before imaging. *Scale bars*: 100 μm. In all samples, the stroma appears to be divided morphologically into an anterior third and posterior two-thirds. Distinct interweaving in the anterior third may be discerned by the through-thickness trajectory of several fibril bundles. Collagen lamellae become thicker toward the posterior of the stroma and run parallel to the stromal surface.
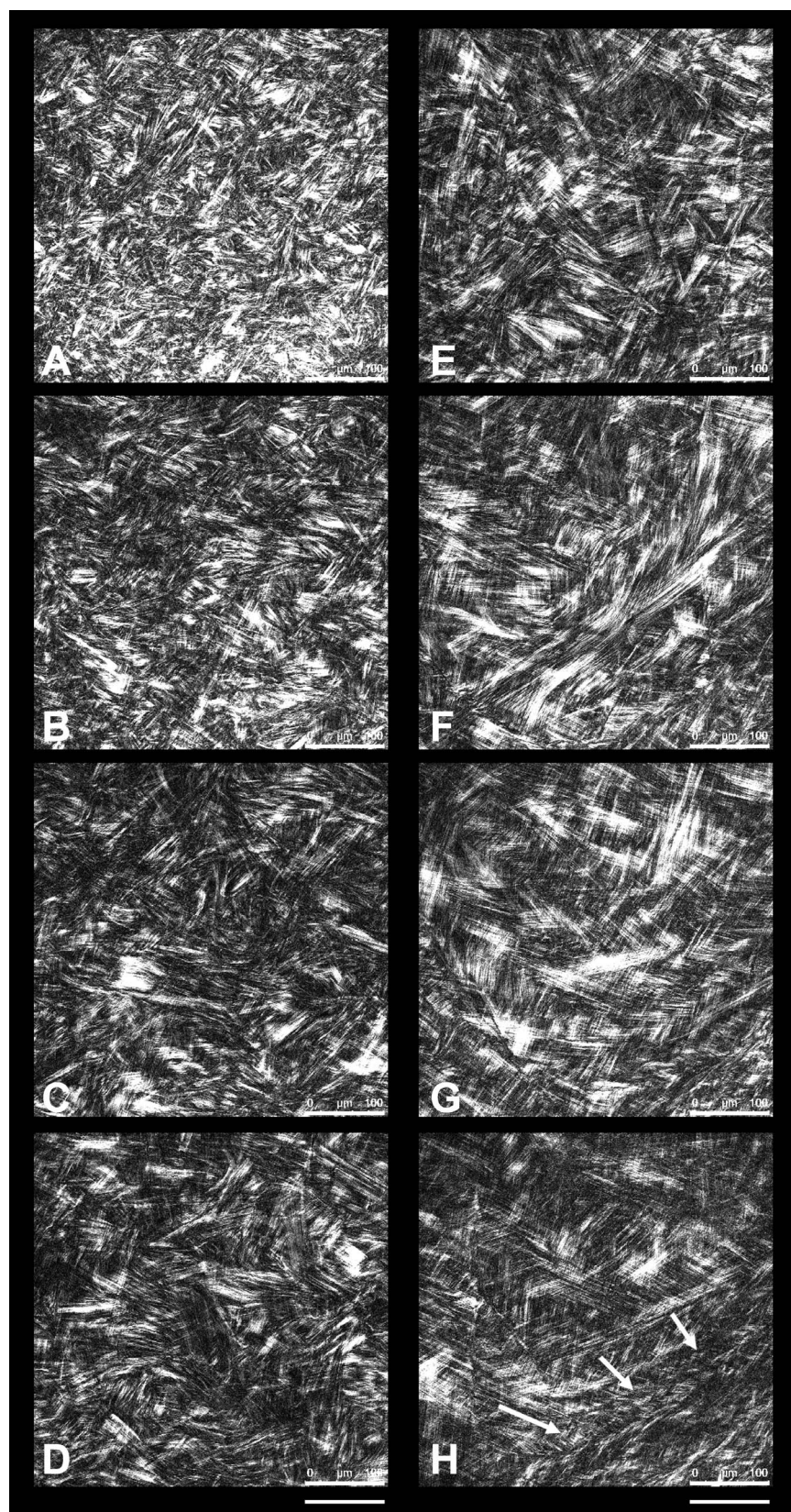
FIGURE 4. Second harmonic generation images of different layers of the human corneal stroma. *Scale bars*: 100 μm. (**A**) Second harmonic generation image at 20-μm depth, showing the collagen fibrils arranging in tiny and short bundles densely interweaved. (**B**) At 60-μm depth, collagen fibril bundles are organized in wider bundles that intersect with each other at different planes. (**C**, **D**) The structural organization of collagen fibril bundles across 130- and 190-μm depth changes in comparison with the most anterior stroma, showing thin and densely packed lamellae. (**E**, **F**) In the mid stroma (250- and 330-μm depth), the collagen lamellae become increasingly wider and thicker. (**G**, **H**) In the posterior stroma (410- and 500-μm depth), the collagen lamellae show a grid-like structure, crossing each other at almost vertical angles; the most posterior lamellae (*white arrows*), lying anteriorly to the Descemet's membrane, are thinner than overlying lamellae.

rate (stress-stiffening response) even in tensile experiments.[27] Overall, the depth-dependent mechanical behavior of the stroma was in fair accordance with that shown in previous work.[6–16] These studies show a 40% to 80% decrease of the elastic modulus from the anterior to posterior stroma of the human cornea, regardless of having applied compressive or tensile stress. However, the tensile strength of collagen fibril bundles is orders of magnitude higher than the compressive strength.[6–16]

Using nanoconical tips, Young's modulus of elasticity was significantly greater than found with microspherical tip; the differences increased with faster application rates. The greater elastic modulus reflects the modulus of the collagen fibril.[9] A decrease of the Young's modulus with increasing stromal depth was found both at 2- and 15-μm/s approach speeds (45%–53% lower) even at the molecular level, though the decrease was less evident than at the tissue level. This difference may be related to the indentation area; a 38-μm spherical tip elicited a mechanical response by a large area of the stroma, in which the depth-dependent influence of the nonelastic ECM components plays an important role. The anisotropic hydration of the stroma, increasing from the anterior to the posterior layers, has been related to the distribution and quantity of different types of ECM components, which offer compressive resistance, across the stroma.[28,29] For the conical nanoindenter, this contribution could be considered negligible, since the tip size was smaller than the average diameter of an individual collagen fiber (30 nm). In addition, the depth-dependent mechanical anisotropy of the stroma could be better emphasized by using a large indentation area, because the anterior stroma shows more cross-linking bonds between collagen and stromal proteins and is less hydrated than the posterior stroma.[1–5] At the nano level, the decrease of E_C with depth could be related to the reduced number of cross-links between collagen fibrils and to local change of type and distribution of proteoglycan core proteins.[28,29]

Previous studies[6–10,19,26] have used AFM to investigate the biomechanical properties of the human corneal stroma. Unfortunately, many experimental differences, including donor age (from 19–93 years), tip size (from 10-nm radius of curvature to 74-μm diameter), spring constant of the cantilever (from 0.06–33 N/m), scan rates (from 2–95 μm/s), indentation depths (from hundreds of nanometers to several micrometers), and stromal region being investigated (from the Bowman' membrane to the Descemet membrane), make data on elastic modulus not comparable between studies. In these previous studies, the elastic modulus was 60% to 70% higher in the anterior portion of the stroma (anterior 70-μm depth) than the posterior one (posterior 30%–60% stromal thickness), consistent with the results of the present work.[7,8,10] The E values collected with nanosized tip (10-nm radius of curvature) were 5 to 10 times greater than they were when collected with microsized tips (1–74 μm diameter) at corresponding stromal regions. Caution should be made when comparing data collected with different scan rates, since the use of lower scan rates (2 μm/s) allows working in an elastic regimen, while the use of faster scan rates introduces hysteresis in the force curves.[8,9]

We correlated the depth-dependent anisotropy of stromal elasticity to images of the human corneal stroma acquired by SHG microscopy. The technique permits imaging of unfixed and unstained tissues at high resolution, thus offering the unique opportunity to visualize the stromal microstructure close to physiological in vivo conditions. The complex patterns of the three-dimensional collagen architecture within the stroma is expected to influence the elasticity of the tissue regionally.[1–5,30] By analysis of reconstructed transverse sections, the corneal stroma could be divided morphologically into an anterior third and posterior two-thirds.[31] The variation of microstructure through the thickness, showing two main structural zones with a boundary at 130- to 160-μm depth correlated strongly with a nonconstant profile of the mechanical properties through the stroma probed with AFM at the tissue level. In this anterior stromal region, the collagen fibrils are organized in bundles that branch and fuse with several other fibrils at different planes. The most anterior collagen fibril bundles insert vertically into Bowman's layer, forming the typical dense mesh of the layer. Bowman's layer and anterior collagen fibril bundles thus form a structural unit to maintain corneal shape and epithelial renewal.[2,9] In the mid and posterior stroma, collagen fibrils are arranged in lamellae that intersect with each other predominantly along the main meridians and show low or no tendency to cross the stroma vertically.

Adequate control of tissue thickness before and during biomechanical experiments provides predictive results of the corneal behavior.[9,32] To avoid any bias due to changes in the hydration state during the experiment, the corneal tissues were kept in 20% dextran solution overnight. Previous studies[7,9,10,13,14,19,26,33,34] indicate that dextran-enriched solutions are effective in avoiding tissue swelling and maintaining corneal hydration during experimentation. In addition, we have previously shown that the corneal thickness remains relatively constant with time in 15% dextran solution, after having the physiological corneal thickness restored in 20% dextran.[19] We found that the corneal thickness and Young's modulus, probed by AFM, was consistent in 15% dextran solution, whereas they increase significantly over time in phosphate-buffered saline, balanced salt solution, and Optisol.[19]

Increasing age is associated with increased corneal tensile and compressive strengths.[23,35] The increase in stiffness has been related to the additional nonenzymatic cross-linking of the stromal proteins. A source of variability in our study could have been introduced by analysis of the posterior stromal surface in tissues of donors with different age (Table 1). Nevertheless, at the tissue level, we found moderate linear correlation between the Young's modulus of elasticity and donor age ($R = 0.50$; $P = 0.05$).

In conclusion, the present results show a depth-dependent mechanical anisotropy of the human corneal stroma both at the tissue and molecular levels. Atomic force microscopy mechanical characterization was valuable for gaining understanding of stromal behavior at both scales. Accurate understanding of the depth-dependent mechanical anisotropy of the corneal stroma at different scales may benefit modelling of corneal behavior and help in the development of biomimetic materials, or for improved scaffolding materials for tissue-engineering applications.[36–38] To thoroughly describe the corneal tissue mechanics, theoretical models encompassing the mesoscopic scales (corneal tissue) between the nanoscopic (corneal molecules) and the macroscopic (eye globe)[14] level are vital. This represents an alternative strategy capable of predicting the properties of human corneal tissue from the bottom-up approach.

References

1. Winkler M, Shoa G, Xie Y, et al. Three-dimensional distribution of transverse collagen fibers in the anterior human corneal stroma. *Invest Ophthalmol Vis Sci*. 2013;54:7293–7301.

2. Morishige N, Takagi Y, Chikama T, Takahara A, Nishida T. Three-dimensional analysis of collagen lamellae in the anterior stroma of the human cornea visualized by second harmonic generation imaging microscopy. *Invest Ophthalmol Vis Sci*. 2011;52:911–915.

3. Meek KM, Blamires T, Elliot GF, Gyi TJ, Nave C. The organisation of collagen fibrils in the human corneal stroma: a synchroton x-ray diffraction study. *Curr Eye Res*. 1987;6:841–846.

4. Komai Y, Ushiki T. The three-dimensional organization of collagen fibrils in the human cornea and sclera. *Invest Ophthalmol Vis Sci*. 1991;32:2244–2258.

5. Muller LJ, Pels E, Vrensen GF. The specific architecture of the anterior stroma accounts for maintenance of corneal curvature. *Br J Ophthalmol*. 2001;85:437–443.

6. Last JA, Liliensiek SJ, Nealey PF, Murphy CJ. Determining the mechanical properties of human corneal basement membranes with atomic force microscopy. *J Struct Biol*. 2009;167:19–24.

7. Dias JM, Ziebarth NM. Anterior and posterior corneal stroma elasticity assessed using nanoindentation. *Exp Eye Res*. 2013;115:41–45.

8. Last JA, Thomasy SM, Croasdale CR, Russell P, Murphy CJ. Compliance profile of the human cornea as measured by atomic force microscopy. *Micron*. 2012;43:1293–1298.

9. Lombardo M, Lombardo G, Carbone G, De Santo MP, Barberi R, Serrao S. Biomechanics of the anterior human corneal tissue investigated with atomic force microscopy. *Invest Ophthalmol Vis Sci*. 2012;53:1050–1057.

10. Dias J, Diakonis VF, Kankariya VP, Yoo SH, Ziebarth NM. Anterior and posterior corneal stroma elasticity after corneal collagen crosslinking treatment. *Exp Eye Res*. 2013;116:58–62.

11. Seifert J, Hammer CM, Rheinlaender J, et al. Distribution of Young's modulus in porcine corneas after riboflavin/UVA induced collagen cross-linking as measured by atomic force microscopy. *PLoS One*. 2014;9:e88186.

12. Kohlhaas M, Spoerl E, Schilde T, Unger G, Wittig C, Pillunat LE. Biomechanical evidence of the distribution of cross-links in corneas treated with riboflavin and ultraviolet A light. *J Cataract Refract Surg*. 2006;32:279–283.

13. Lombardo M, Serrao S, Rosati M, Ducoli P, Lombardo G. Biomechanical changes of the human cornea following transepithelial corneal cross-linking using iontophoresis. *J Cataract Surg*. 2014;40:1706–1715.

14. Lombardo M, Serrao S, Rosati M, Lombardo G. Analysis of the viscoelastic properties of the human cornea using Scheimpflug imaging in inflation experiment of eye globes. *PLoS One*. 2014;9:e112169.

15. Dupps WJ, Netto MV, Herekar S, Krueger RR. Surface wave elastometry of the cornea in porcine and human donor eyes. *J Refract Surg*. 2007;23:66–75.

16. Scancelli G, Pineda R, Yun SH. Brillouin optical microscopy for corneal biomechanics. *Invest Ophthalmol Vis Sci*. 2013;53:185–190.

17. Petsche SJ, Chernyak D, Martiz J, Levenston ME, Pinsky PM. Depth-dependent transverse shear properties of the human corneal stroma. *Invest Ophthalmol Vis Sci*. 2012;53:873–880.

18. Butt HJ, Cappella B, Kappl M. Force measurements with the atomic force microscope: technique, interpretation and applications. *Surf Sci Rep*. 2005;59:1–152.

19. Dias J, Ziebarth NM. Impact of hydration media on ex vivo corneal elasticity measurements [published online ahead of print January 19, 2015]. *Eye Contact Lens*.

20. Ebenstein DM, Pruitt LA. Nanoindentation of biological materials. *NanoToday*. 2006;1:26–33.

21. Gibson CT, Watson GS, Myhra S. Determination of the spring constants of probes for force microscopy/spectroscopy. *Nanotechnology*. 1996;7:259–262.

22. Tortonese M, Kirk M. Characterization of application specific probes for SPMs. *Proc SPIE*. 1997;3009:53–60.

23. Knox Cartwright NE, Tyrer JR, Marshall J. Age-related differences in the elasticity of the human cornea. *Invest Ophthalmol Vis Sci*. 2011;52:4324–4329.

24. Poggi MA. A method for calculating the spring constant of atomic force microscopy cantilevers with a nonrectangular cross section. *Anal Chem*. 2005;77:1192–1195.

25. Ahearne M, Yang Y, Then KY, Liu KK. An indentation technique to characterize the mechanical and viscoelastic properties of human and porcine corneas. *Ann Biomed Eng*. 2007;35:1608–1616.

26. Labate C, De Santo MP, Lombardo G, Lombardo M. Understanding of the viscoelastic response of the human corneal stroma induced by riboflavin/UV-A cross-linking at the nano level. *PLoS One*. 2015;10:e0122868.

27. Elsheikh A, Wang D, Pye D. Determination of the modulus of elasticity of the human cornea. *J Refract Surg*. 2007;23:808–818.

28. Muller LJ, Pels E, Schurmans L, Vrensen G. A new three-dimensional model of the organization of proteoglycans and collagen fibrils in the human corneal stroma. *Exp Eye Res*. 2004;78:493–501.

29. Wilson G, O'Leary DJ, Vaughan W. Differential swelling in compartments of the corneal stroma. *Invest Ophthalmol Vis Sci*. 1984;25:1105–1111.

30. Winkler M, Chai D, Kriling S, et al. Nonlinear optical macroscopic assessment of 3-D corneal collagen organization and axial biomechanics. *Invest Ophthalmol Vis Sci*. 2011;2:8818–8827.

31. Ruberti JW, Roy AS, Roberts CJ. Corneal structure and function. *Annu Rev Biomed Eng*. 2011;13:269–295.

32. Hatami-Marbini H, Etebu E. Hydration dependent biomechanical properties of the corneal stroma. *Exp Eye Res*. 2013;116:47–54.

33. Hamaoui M, Tahi H, Chapon P, et al. Corneal preparation of eye bank eyes for experimental surgery. *Cornea*. 2001;20:317–320.

34. Borja D, Manns F, Lamar P, Rosen A, Fernandez V, Parel JM. Preparation and hydration control of corneal tissue strips for experimental use. *Cornea*. 2004;23:61–66.

35. Elsheikh A, Wang D, Brown M, Rama P, Campanelli M, Pye D. Assessment of corneal biomechanical properties and their variation with age. *Curr Eye Res*. 2007;32:11–19.

36. Studer H, Larrea X, Riedwyl H, Büchler P. Biomechanical model of human cornea based on stromal microstructure. *J Biomech*. 2010;43:836–842.

37. Thomasy SM, Raghunathan VK, Winkler M, et al. Elastic modulus and collagen organization of the rabbit cornea: epithelium to endothelium. *Acta Biomater*. 2014;10:785–791.

38. Ruberti JW, Zieske JD. Prelude to corneal tissue engineering: gaining control of collagen organization. *Prog Ret Eye Res*. 2008;27:549–577.